Arabian Journal of Chemistry (2020) 13, 3624–3632

King Saud University

Arabian Journal of Chemistry

www.ksu.edu.sa
www.sciencedirect.com

ORIGINAL ARTICLE

Efficient photocatalytic treatment of sugar mill wastewater with 2%Ag_3PO_4/Fe/GTiP nanocomposite

Noor Ahmed Nahyoon [a], Lifen Liu [a,*], Waseem Saleem [b], Sarwan Ahmed Nahyoon [b], Kané Rabé [a]

[a] *Key Laboratory of Industrial Ecology and Environmental Engineering (MOE), School of Environmental Science and Technology, Dalian University of Technology, Dalian 116024, China*
[b] *Center of Advance Studies in Water, Mehran University of Engineering and Technology, Jamshoro, Pakistan*

Received 8 October 2019; accepted 13 December 2019
Available online 26 December 2019

KEYWORDS

Photocatalysis;
Sugar mill;
2%Ag_3PO_4/Fe/GTiP;
Decolorization;
COD removal

Abstract The large amount of colored substances exist in the sugar mills wastewater that give higher organic load to the effluent. Therefore, a novel study of sugar mill wastewater treatment was carried out under photocatalysis by using a nanocomposite of silver phosphate-iron-graphene oxide-titanium phosphate (Ag_3PO_4/Fe/GTiP). The catalyst was prepared by simple chemical process with 2% content of Ag_3PO_4 to Fe/GTiP. The light, catalyst dosage, pH, and scavenger impacts on the decolorization and chemical oxygen demand (COD) removal from the sugar mill wastewater were observed. The highest decolorization and COD removal of 85.02% and 80.3% was achieved under pH-1 by using 50 W visible halogen light at catalyst dosage of 100 mg/75 ml in 200 min. The excellent recycled results were observed up to four cycles. The obtained results proves that this catalyst has high photocatalytic efficiency to treat the sugar mill wastewater.

1. Introduction

Water pollution is globally one of the serious problems. The severe contamination of most of the fresh water resources with untreated municipal and industrial water has been caused due to rapid industrialization, population growth, urbanization (Mane et al., 2015). It is absolutely necessary to avoid polluting freshwater bodies by treating and reusing wastewater (Shivayogimath and Jahagirdar, 2013). There are enormous implications for human health and social life in design and operation of built environment. For environmental quality standard, the affordable, innovative, and appropriate development solutions are required through which positive financial and social influences can be maximized and undesirable effects on environment can be minimized. In the future, to prevent

* Corresponding author.
Peer review under responsibility of King Saud University.

ELSEVIER Production and hosting by Elsevier

https://doi.org/10.1016/j.arabjc.2019.12.004

environmental pollution and continue functioning under no depletion or overloading critical resources such type of environmental solutions will be beneficial (see Table 1).

Pakistan is the 5thth largest sugar producing country in the world (Nazir et al., 2013). In the process, for every ton of can crush, nearly 1000 L of wastewater is produced. The untreated discharged wastewater of sugar industry is unfit for both human and aquatic uses because high oxygen demand wastewater lead to the depletion of dissolved oxygen content in the water bodies (Qureshi et al., 2015). By discharging untreated wastewater in the open yard, the existing organic solids in the wastewater clog the soil pores (Reddy et al., 2015). Therefore, it is challenging task to purify sugar industry wastewater due to stringent discharge standards for the environmental protection.

Table 1 The kinetic parameters under catalyst dosage of 50 mg/75 ml for treated sugar mill wastewater under visible light.

Name of catalyst	K(min^{-1})	R^2
TiP	0.019	0.957
GTiP	0.035	0.986
Fe/GTiP	0.06	0.995
2%Ag_3PO_4/Fe/GTiP	0.089	0.994

To solve the sugar industry wastewater pollution problems, mostly physico-chemical and biological treatment methods have been adopted (Kumar and Srikantaswamy, 2015). The high organic removal with certain bacteria and fungi have been achieved in biological treatment but color removal efficiencies are very low (Miranda et al., 1996; Miyata et al., 2000). Recently, advanced oxidation processes (AOPs) have been focused to remove significant color. The AOP is defined as the process of generating sufficient hydroxyl radicals to be able to oxidize organic substances existing in the wastewater (Apollo et al., 2014). In such AOPs, photocatalysis has emerged as possible strategy for water remediation involving the eradication of aqueous phase contaminants (Raizada et al., 2019). In photocatalysis, titanium dioxide (TiO_2) has been used as photocatalyst a for water splitting since 1972 (Raizada et al., 2019), due to owing characteristics of non-toxicity, low cost, good chemical stability, and high photocatalytic activity (Liu et al., 2016). The wide band gap (~3.2 eV), only active under ultraviolet light (2–4% of solar spectrum), slow oxidation, and low quantum efficiency make its use

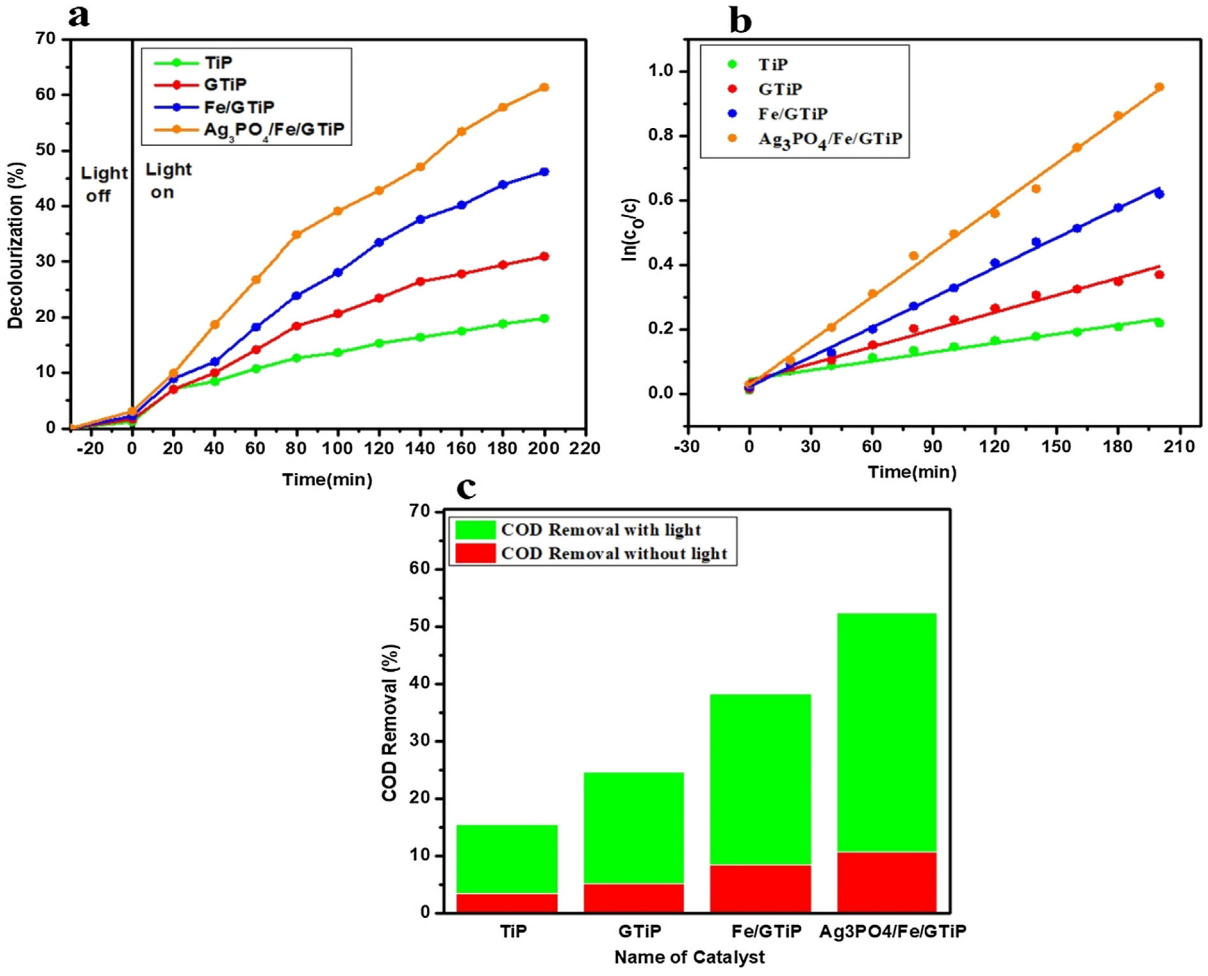

Fig. 1 (a) Decolorization of sugar mill wastewater treated with catalyst dosage of 50 mg/75 ml TiP, GTiP, Fe/GTiP, and 2%Ag_3PO_4/Fe/GTiP under visible light at initial pH-9.5 (b) The kinetic fitting curves of sugar mill wastewater treated with TiP, GTiP, Fe/GTiP, and 2% Ag_3PO_4/Fe/GTiP under visible light at initial pH-9.5 (c) The COD removal under visible light and without light at initial pH-9.5.

limited in photocatalysis (Rabé et al., 2019a; Raizada et al., 2020). Hence, to make it active under visible or sunlight, new photocatalytic materials are required either by compositing with other catalysts or by replacing TiO_2 (Liu et al., 2016; Rabé et al., 2019).

Generally, for an efficient photodegradation process, adsorption of organic pollutant is necessary. The combination of graphene and its derivatives with semiconductors has recently emerged as a simple strategy to increase the activity and stability of wastewater treatment photocatalytic system (Shandilya et al., 2018). Graphene and its derivatives appears as potential candidate for the construction of the supported photocatalyst (Singh et al., 2019). In the photocatalytic application of wastewater treatment, graphene oxide (GO) is widely used due to its outstanding electronic properties, large surface area, high carrier mobility, and several oxygen containing functional groups (Thebo et al., 2018). Various doping strategies of GO with metal ions, non-metal ions, have been carried out to extend the light absorption of the photocatalysts from UV to visible range (Mecha et al., 2017). The electronic and photocatalytic properties of a semiconductor photocatalyst are changed with metal-ion doping. The dopant shifts the absorption from UV to visible range wavelengths and enhances photo-reactions. Among all methods, the formation of heterostructure between two semiconductors is considered the most suitable approach for expanding the spectrum of solar light absorption and improving the photodegradation of aqueous phase pollutants (Singh et al., 2019). Heterojunction design has recently emerged as a novel technique to solve conventional photocatalyst defects, resulting in the technology of composite photocatalyst's desired electronic properties to effectively isolate the photogenerated charge carriers (Rabé et al., 2019b; Raizada et al., 2017). The most effective strategy for minimizing the recombination of photogenerated electrons and holes is heterojunction formation with another semiconductor with well-balanced valence and conduction band potential (Raizada et al., 2019). To enhance the photocatalytic degradation efficiency, graphene-based nanocomposites GO/Ag/PO (Yang et al., 2013), Fe_3O_4/rGO/TiO_2 (Wang et al., 2017), ZnS-CdS/GO, CdS/g-C_3N_4/1 wt% GO (Li et al., 2018), have been reported. Also, the superlative visible light driven behavior of photocatalysts based on Ag_3PO_4 has drawn attention to their use in the degradation of organic/inorganic pollutants. Therefore, for the photocatalytic water splitting, Ag_3PO_4/Ag/graphene/g-C_3N_4 composite has also been studied (Raizada et al., 2019). On the other hand, phosphate-based composites

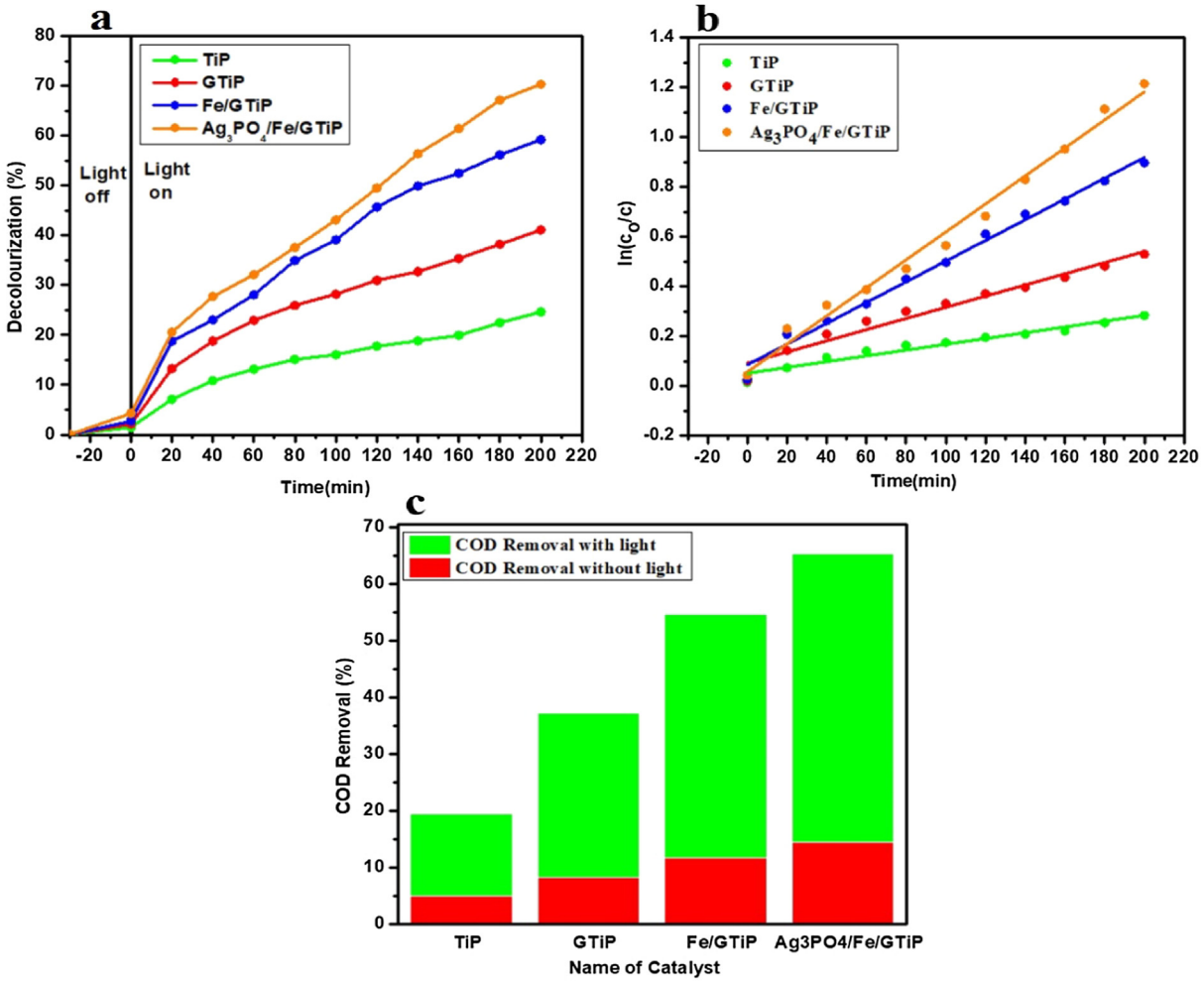

Fig. 2 (a) Decolorization of sugar mill wastewater treated with catalyst dosage of 100 mg/75 ml TiP, GTiP, Fe/GTiP, and 2%Ag_3PO_4/Fe/GTiP under visible light at initial pH-9.5 (b) The kinetic fitting curves of sugar mill wastewater treated with TiP, GTiP, Fe/GTiP, and 2%Ag_3PO_4/Fe/GTiP under visible light at initial pH-9.5 (c) The COD removal under visible light and without light at initial pH-9.5.

are widely used for various applications including water treatment and energy storage application (Hung et al., 2016; Kim et al., 2017; Martín-Yerga et al., 2017; Park et al., 2016; Zhao et al., 2017). Titanium phosphate (TiP) have replaced TiO_2 and known as high performance inorganic cation exchange material (Wang et al., 2014). It has high photooxidation and reduction capability, low fabrication cost, good chemical stability, and non-toxicity (Ao et al., 2016).

In this study, the decolorization and chemical oxygen demand (COD) removal from sugar industry wastewater have been carried out by using AOPs (Photocatalysis) in which heterojunction composite catalyst of silver phosphate-iron-graphene oxide-titanium phosphate ($2\%Ag_3PO_4$/Fe/GTiP) (Nahyoon et al., 2019) have been utilized.

Table 2 The kinetic parameters under catalyst dosage of 100 mg/75 ml for treated sugar mill wastewater under visible light.

Name of catalyst	K(min^{-1})	R^2
TiP	0.024	0.961
GTiP	0.046	0.968
Fe/GTiP	0.083	0.993
$2\%Ag_3PO_4$/Fe/GTiP	0.11	0.989

2. Material and methods

The wastewater sample of the operational sugar mill was collected from Matiari Sugar mill, District Matiari, Sindh, Pakistan during the crushing season 2018–19.

2.1. Preparation of catalyst

Graphene oxide (GO), titanium phosphate (TiP), graphene oxide-titanium phosphate (GTiP), iron-graphene oxide-titanium phosphate (Fe/GTiP) (Nahyoon et al., 2018), and silver phosphate- iron-graphene oxide-titanium phosphate (2% Ag_3PO_4/Fe/GTiP) were prepared according to our previous study (Nahyoon et al., 2019).

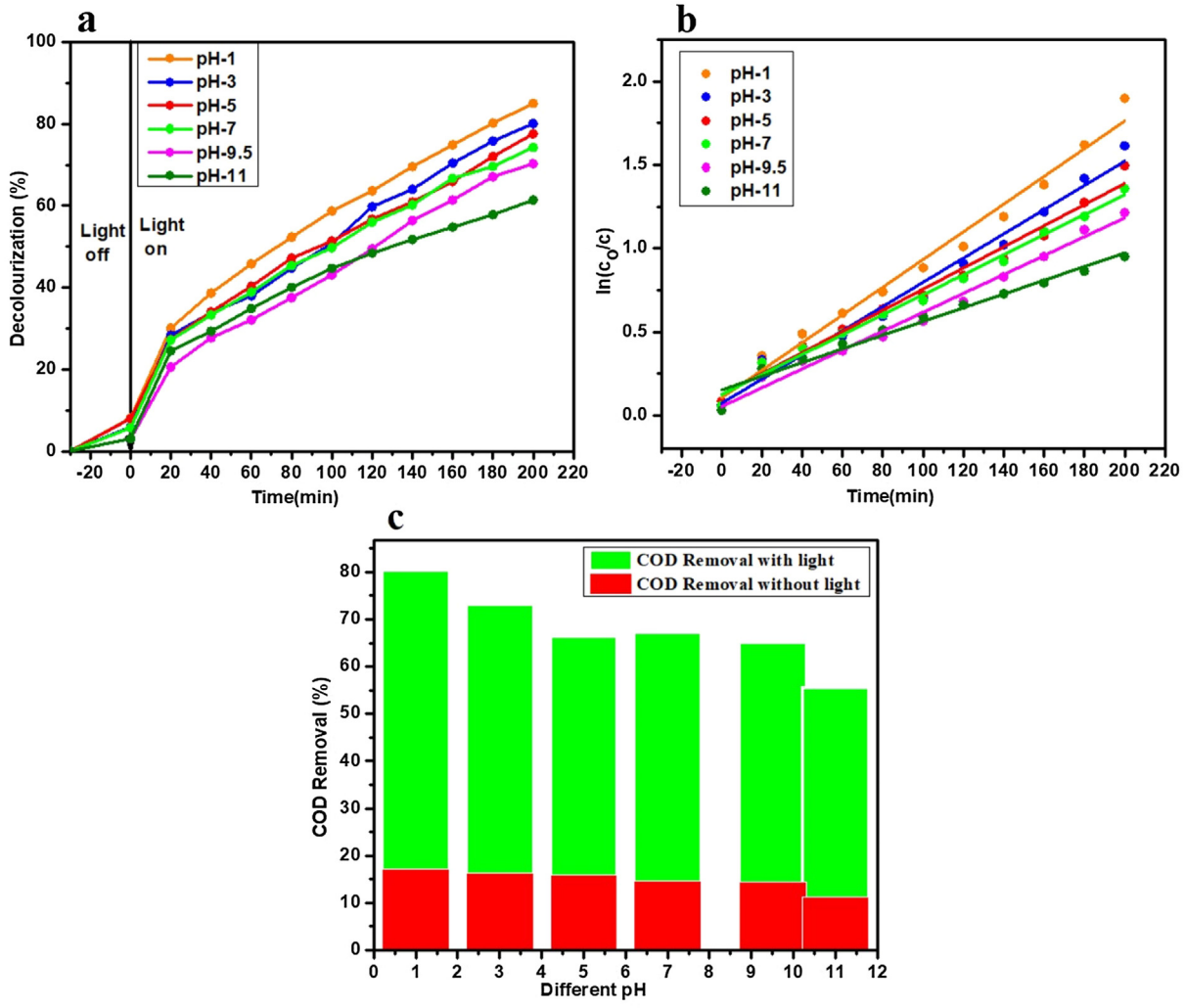

Fig. 3 (a) Decolorization of sugar mill wastewater treated with $2\%Ag_3PO_4$/Fe/GTiP catalyst dosage of 100 mg/75 ml under visible light at different pH (b) The kinetic fitting curves of sugar mill wastewater treated with $2\%Ag_3PO_4$/Fe/GTiP under visible light at different pH (c) The COD removal with $2\%Ag_3PO_4$/Fe/GTiP under visible light and without light at different pH.

2.2. Photocatalytic study

The wastewater samples were used in photocatalysis by using different catalyst dosage of 2%Ag_3PO_4/Fe/GTiP in 75 ml of wastewater irradiating with 50-watt visible halogen lamp for decolorization and COD removal. Initially the catalyst was added in the wastewater sample and sonicated for 2–3 min. Then the suspension was magnetically stirred for 30 min in dark, after that 5 ml of the suspension was taken. Then it was aerated and irradiated with visible light. At the time interval of every 20 min, 5 ml of suspension was collected. Finally, from the collected 5 ml suspension, 1 ml was used for decolorization by diluting with 4 ml deionized water and 4 ml was used for COD removal. The diluted samples for decolorization were centrifuged at 8000 rpm for 2 min and measured in terms of absorbance at wavelength of 430 nm (Sahu, 2016) in UV–vis spectrophotometer. The COD was measured by potassium dichromate method based on China National Standard GB 11914-89 (Liu et al., 2010). The decolorization efficiency and COD removal was calculated by Eqs. (1) and (2).

Table 3 The kinetic parameters under 2%Ag_3PO_4/Fe/GTiP catalyst dosage of 100 mg/75 ml for treated sugar mill wastewater under visible light at different pH.

pH	K(min^{-1})	R^2
1	0.163	0.986
3	0.142	0.983
5	0.126	0.986
7	0.119	0.992
9.5	0.105	0.983
11	0.071	0.946

$$\text{Decolorization Efficiency } (\%) = C_o - \frac{C_t}{C_O} * 100 \quad (1)$$

where Co represent to initial concentration of wastewater and C_t represent to final concentration of wastewater at time t.

$$\text{COD Removal Efficiency } (\%) = \frac{1}{V_o} * 8000 * (V_o - V_t) \quad (2)$$

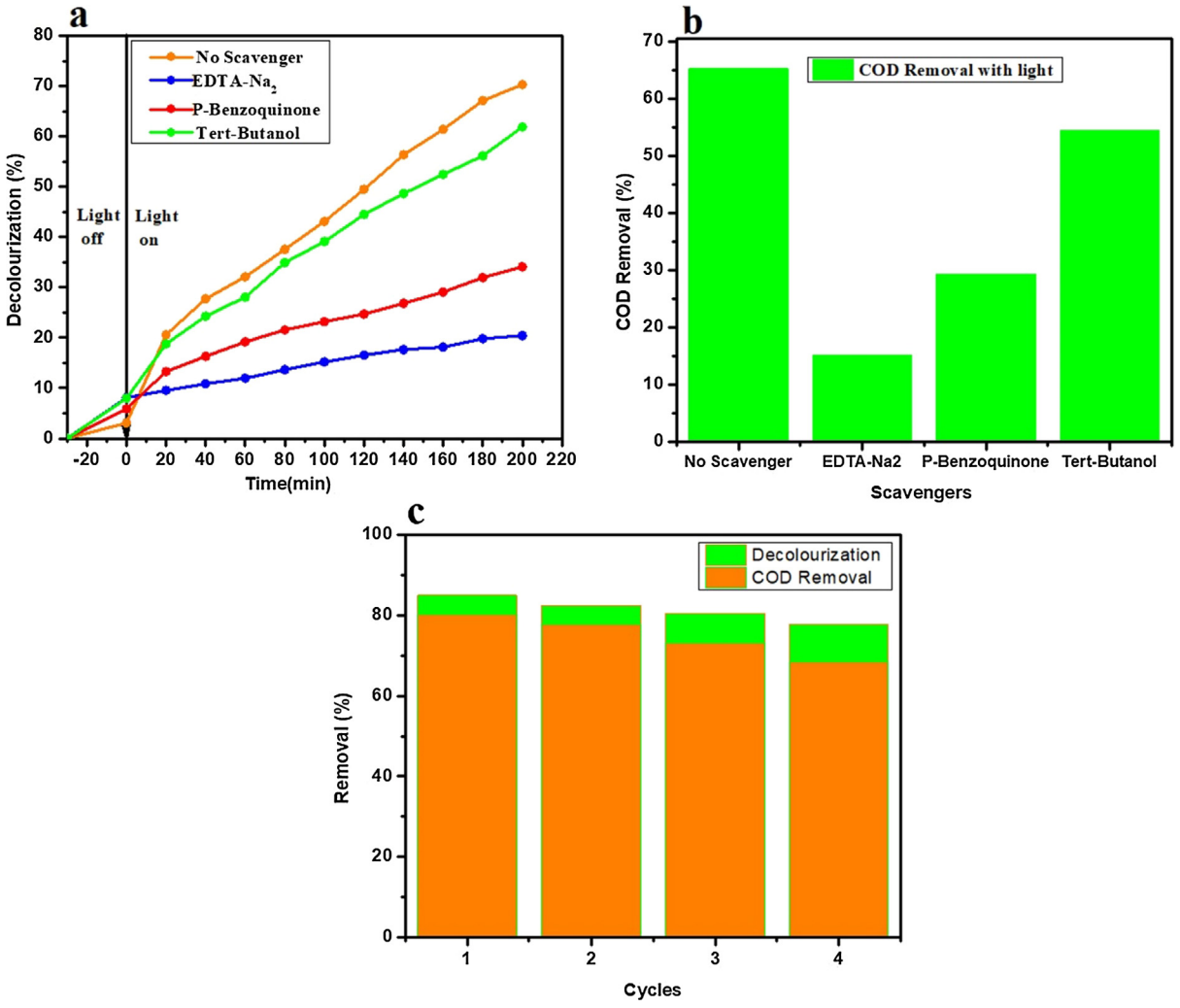

Fig. 4 (a) The scavenger effect on the decolorization of the sugar mill wastewater under visible light at initial pH of 9.5 (b) The scavenger effect on the COD removal of the sugar mill wastewater under visible light at initial pH of 9.5 (c) The recyclability performance for the decolorization and COD removal under pH −1 under 2% Ag_3PO_4/Fe/GTiP.

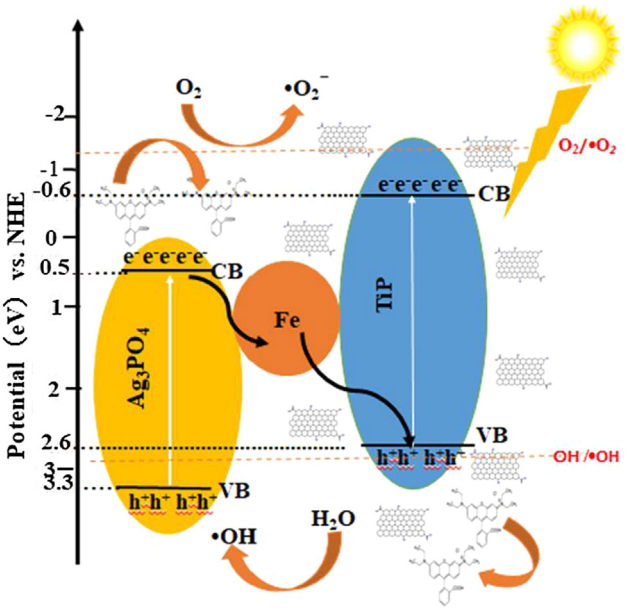

Fig. 5 Schematic photocatalytic mechanism for 2% Ag_3PO_4/Fe/GTiP nanocomposite.

where $1/V_o = C$, representing the concentration of $(NH_4)_2(SO_4)_2$ used for blank sample and V_t is the concentration of $(NH_4)_2(SO_4)_2$ used for the sample.

3. Result and discussion

The characterizations of the prepared heterojunction catalyst 2%Ag_3PO_4/Fe/GTiP are reported in our previous study (Nahyoon et al., 2019). The photocatalytic performance of 2%Ag_3PO_4/Fe/GTiP was evaluated by degrading sugar mill wastewater under visible light of 50-watt halogen lamp. At initial pH-9.5 of wastewater, by using the catalyst dosage 50 mg/75 ml, the obtained decolorization under TiP, GTiP, Fe/GTiP, and 2%Ag_3PO_4/Fe/GTiP were 19.8, 30.95, 46.2, and 61.4% in 200 min as shown in Fig. 1a. The kinetic linear fitting curves follow the Langmuir-Hinshelwood apparent 1st order kinetic model shown in Fig. 1b. While, decolorization under without light was 6.26, 7.24, 11.27, and 14.46% with same initial pH, time duration, and catalyst dosage as shown in Fig. S1. The initial COD was 3942 mg/l. The COD removal at above same conditions under visible light at TiP, GTiP, Fe/GTiP, and 2%Ag_3PO_4/Fe/GTiP was 15.4%, 24.6, 38.3, and 52.4%. While, under without light COD removal was 3.42, 5.2, 8.5, and 10.7% as shown in Fig. 1c.

By increasing the catalyst dosage up to 100 mg/75 ml, the obtained decolorization at initial pH-9.5 with TiP, GTiP, Fe/GTiP, and 2%Ag_3PO_4/Fe/GTiP were 24.63, 41.1, 59.19, and 70.29% in 200 min under visible light of 50-watt as shown in Fig. 2a. While under without light, following the same initial pH and catalyst dosage, the decolorization was 9.27, 12.56,

Table 4 Comparison of the current study with other methods reported previously for the treatment of sugar mill wastewater.

S.No	Process	COD Removal (%)	Color Removal (%)	Time (min)	Ref.
1	Electrochemical	90	93.5	120	(Sahu, 2017)
2	Thermolysis	75.6	79.2	240	(Sahu et al., 2018)
3	Thermal + Electrocoagulation	97.8	99.7	240	(Sahu et al., 2018)
4	Photocatalysis	Not measured	97	350	(Apollo et al., 2014)
5	Electroxidation	63.1	99.9	420	(Capunitan et al., 2008)
6	Electrocoagulation	18.5	71.2	480	(Capunitan et al., 2008)
7	Photocatalysis	80.3	85.02	200	Current Study

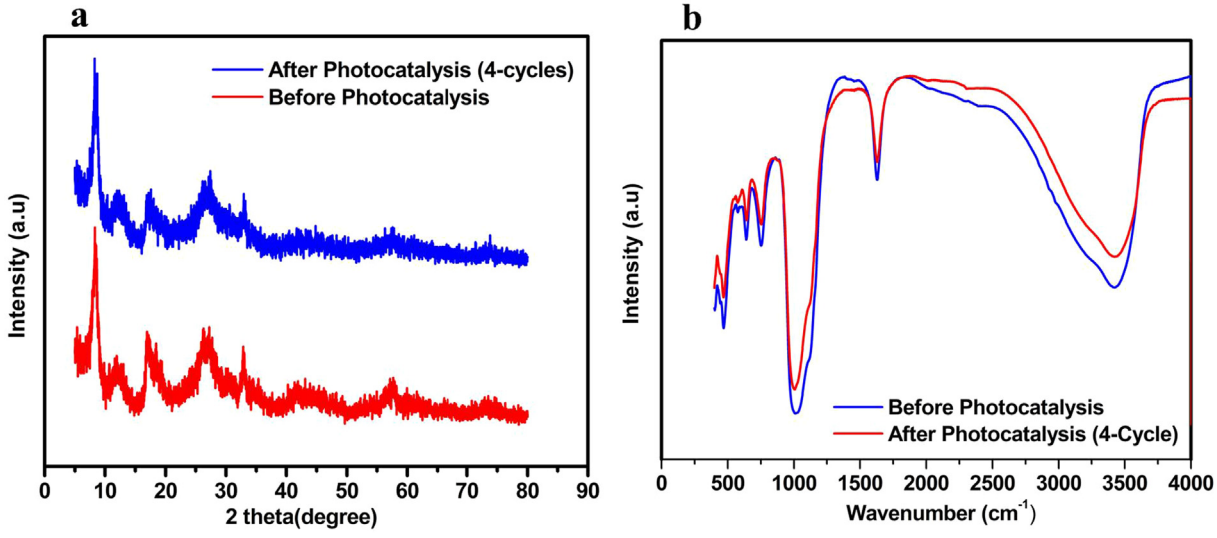

Fig. 6 (a) XRD (b) FTIR spectra for 2%Ag_3PO_4/Fe/GTiP before and after 4 photocatalytic cycles.

15.91, and 19.85% as shown in Fig. S2. The COD removal with TiP, GTiP, Fe/GTiP, and 2%Ag_3PO_4/Fe/GTiP under visible light was 19.5, 37.23, 54.53, and 65.21%. While, under without light it was 5, 8.2, 11.7, and 14.5% as shown in Fig. 2c. The kinetic linear fitting curves for the treatment under 100 mg catalyst dosage are shown in Fig. 2b. The kinetic parameters of (100 mg/75 ml) treated sugar mill wastewater under visible light are illustrated in Table 2.

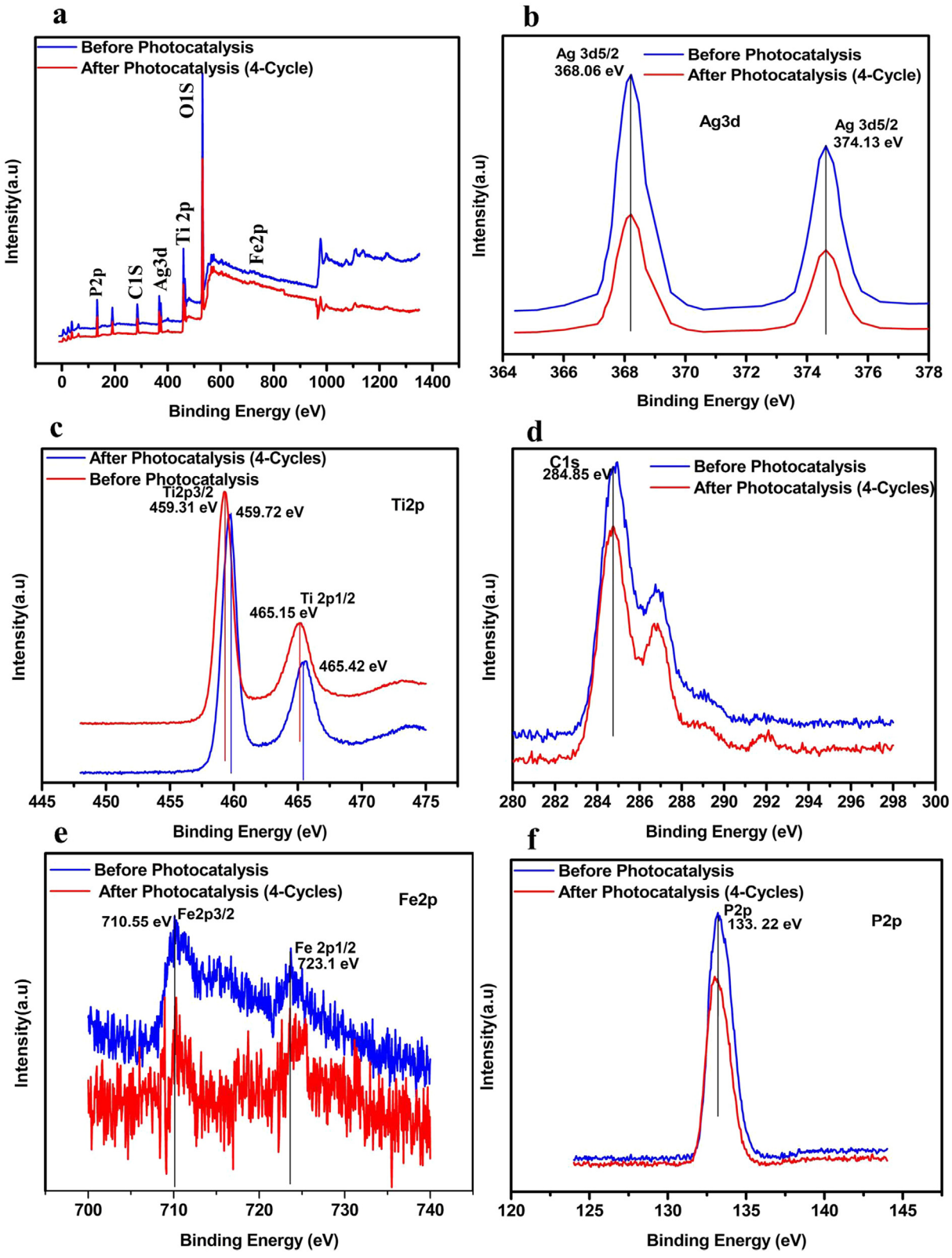

Fig. 7 (a) XPS spectra for 2%Ag_3PO_4/Fe/GTiP before and after 4 photocatalytic cycles.

The pH effect on the decolorization and COD removal was studied by using heterojunction catalyst 2%Ag_3PO_4/Fe/GTiP. The decolorization with 50-watt visible light under 100 mg/75 ml catalyst dosage at different pH of 1, 3, 5, 7, 9.5(initial), and 11 was 85.02, 80.07, 77.57, 74.27, 70.29, and 61.40% in 200 min as shown in Fig. 3a. While, under without light it was 23.42, 22.91, 20.17, 20.29, 19.85, 17.24%. The COD removal under visible light keeping the above same conditions was 80.3, 73.2, 66.35, 67.31, 65.21, and 55.65%. While, under without light the COD removal was 17.13, 16.38, 15.8, 14.7, 14.5, and 11.23% as shown in Fig. 3c. The kinetic linear fitting curves for the treatment under 100 mg catalyst dosage at different pH are shown in Fig. 3b. The kinetic parameters of (100 mg/75 ml) treated sugar mill wastewater at different pH under visible light are illustrated in Table 3.

Further, the photocatalytic mechanism was studied for the decolorization and COD removal at initial pH of 9.5 by using 0.05 M/L scavenger concentration of EDTA-Na_2, p-benzoquinone, and *tert*-butanol separately. The obtained decolorization by irradiating with 50-Watt visible light under EDTA-Na_2, p-benzoquinone, and *tert*-butanol with 2%Ag_3PO_4/Fe/GTiP catalyst dosage of 100 mg/75 was 20.41, 34.08, and 61.88% which is less than 70.29% of without any scavenger as shown in Fig. 4a. While, the COD removal was 20.41, 34.08, 61.88% which is less than 70.29% under absence of any scavenger as shown in Fig. 4b. The obtained results illustrate that there is significant role of irradiated $O_2^{\cdot-}$ and h^+ and in the photocatalytic system contribute the most to the Ag_3PO_4/Fe/GTiP. EDTA shows less influence which demonstrates the less importance of $OH^{\cdot}$. By the electron-hole ($e^- - h^+$) separation between the valance and conduction band, the probable mechanism of Ag_3PO_4/Fe/GTiP for the sugar mill wastewater photodegradation could be explained as represented in Fig. 5. The excitation of the electron takes place, when the sunlight falls on the surface of Ag_3PO_4/Fe/GTiP, after absorption of photon from lowest energy valence band. The movement of the excited electrons in the nanocomposite takes place from the valence to conduction band. In result, on the surface of the Ag_3PO_4/Fe/GTiP composite, the separation of electron-hole pairs takes place. Within the valence band of nanocomposite, the electron hole pairs are generated, which are further captured by water molecules and results the formation of active hydroxyl radicals ($OH^{\cdot}$**).** The Ag_3PO_4/Fe/GTiP composite plays an excellent role in the photocatalytic degradation of sugar mill wastewater. The reusability performance of 2%Ag_3PO_4/Fe/GTiP catalyst for the sugar mill wastewater was carried out at pH-1. After four cycles, the decolorization was 85.02, 82.3, 80.5, and 77.7%. While, COD removal was 80.3, 77.7, 73.2, and 68.4% as represented in Fig. 4c. The minor decrease in result was due to loss of catalyst in washing process. The catalyst proved good photocatalytic performance. Finally, the current study results are compared with other used methods for the treatment of sugar industry wastewater reported previously as illustrated in Table 4. The stability of photocatalyst has also been compared in terms of XRD, FTIR and XPS before and after four photocatalytic cycles as shown in Fig. 6 and Fig. 7.

4. Conclusion

The treatment of sugar mill wastewater under photocatalysis was carried out by using visible light driven 2%Ag_3PO_4/Fe/GTiP nanocomposite. The catalyst was synthesized by simple chemical process. The light, catalyst dosage, pH, and scavenger effect on the decolorization and COD removal from sugar mill wastewater were studied. The decolorization and COD removal at initial pH-9.5 under visible light of 50 W and without light with catalyst dosage of 50 mg/ 75 ml were 61.4% & 52.4% and 14.46% & 10.7% in 200 min. With catalyst dosage of 100 mg/ 75 ml the decolorization and COD removal under light and without light were 70.29% & 65.21% and 19.85% and 14.5%. At pH-1, the decolorization and COD removal with catalyst dosage of 100 mg/ 75 ml under light and without light were 85.02% & 23.42% and 80.3% & 17.3%. The decolorization and COD removal under scavenger were less than without scavenger. After four recycles use, the good performance of the catalyst was found under photocatalysis. The obtained results demonstrate that this catalyst can effectively treat the sugar mill wastewater.

Acknowledgement

The current study was carried out with the support of China National science foundation (Project No. 21677025) and the authors are thankful to Sindh Environmental Protection Agency, Government of Sindh, Pakistan and Center of Advance Studies in Water, Mehran University of Engineering and Technology, Jamshoro, Pakistan for completion of research work at their laboratories.

Declaration of Competing Interest

There is no conflict of interest.

Appendix A. Supplementary material

Supplementary data to this article can be found online at https://doi.org/10.1016/j.arabjc.2019.12.004.

References

Ao, Y., Bao, J., Wang, P., Wang, C., Hou, J., 2016. Bismuth oxychloride modified titanium phosphate nanoplates: a new pn type heterostructured photocatalyst with high activity for the degradation of different kinds of organic pollutants. J. Colloid Interface Sci. 476, 71–78.

Apollo, S., Onyongo, M.S., Ochieng, A., 2014. UV/H_2O_2/TiO_2/zeolite hybrid system for treatment of molasses wastewater. Iranian J. Chem. Chem. Eng. (IJCCE) 33 (2), 107–117.

Capunitan, J.A. et al, 2008. Decolorization and chemical oxygen demand (COD) reduction of sugar refinery spent ion-exchange-process (SIEP) effluent by electrochemical treatment methods. Philippine Agricultural Scientist (Philippines).

Hung, T.-F., Lan, W.-H., Yeh, Y.-W., Chang, W.-S., Yang, C.-C., Lin, J.-C., 2016. Hydrothermal synthesis of sodium titanium phosphate nanoparticles as efficient anode materials for aqueous sodium-ion batteries. ACS Sustain. Chem. Eng. 4 (12), 7074–7079.

Kim, Y., Kim, H.-C., Lee, J., Lee, S.-H., Kwon, K.-Y., 2017. Morphological change and photocatalytic activity of titanium phosphates. J. Photochem. Photobiol., A 338, 146–151.

Kumar, D.S., Srikantaswamy, S., 2015. Evaluation of effluent quality of a sugar industry by using physico-chemical parameters. Int. J. Adv. Res. Eng. Appl. Sci. 4 (1), 16–25.

Li, X., Shen, R., Ma, S., Chen, X., Xie, J., 2018. Graphene-based heterojunction photocatalysts. Appl. Surf. Sci. 430, 53–107.

Liu, W., Liu, Q., Li, X., Song, Y., Cao, W., 2010. Photocatalytic degradation of coking wastewater by nanocrystalline (Fe, N) co-doped TiO_2 powders. Sci. China Technol. Sci. 53 (6), 1477–1482.

Liu, Y., Liu, L., Yang, F., 2016. Energy-efficient degradation of rhodamine B in a LED illuminated photocatalytic fuel cell with anodic Ag/AgCl/GO and cathodic $ZnIn_2S_4$ catalysts. RSC Adv. 6 (15), 12068–12075.

Mane, P., Chaudhari, R., Papade, S., Kadam, D., Mahabare, K., Konde, V., Birajdar, F., 2015. Study on bioremediated sugar industry effluent for Irrigation: an evaluative study on the biochemical attributes of Vigna radiata under laboratory conditions. Ann. Biol. Res. 6 (6), 26–32.

Martín-Yerga, D., Carrasco-Rodríguez, J., Fierro, J.L.G., Alonso, F. J.G., Costa-García, A., 2017. Copper-modified titanium phosphate nanoparticles as electrocatalyst for glucose detection. Electrochim. Acta 229, 102–111.

Mecha, A.C., Onyango, M.S., Ochieng, A., Momba, M.N., 2017. Evaluation of synergy and bacterial regrowth in photocatalytic ozonation disinfection of municipal wastewater. Sci. Total Environ. 601, 626–635.

Miranda, M.P., Benito, G.G., San Cristobal, N., Nieto, C.H., 1996. Color elimination from molasses wastewater by Aspergillus niger. Bioresour. Technol. 57 (3), 229–235.

Miyata, N., Mori, T., Iwahori, K., Fujita, M., 2000. Microbial decolorization of melanoidin-containing wastewaters: combined use of activated sludge and the fungus Coriolus hirsutus. J. Biosci. Bioeng. 89 (2), 145–150.

Nahyoon, N.A., Liu, L., Rabé, K., Nahyoon, S.A., Abro, A.H., Yang, F., 2019. Efficient degradation of rhodamine B with sustainable electricity generation in a photocatalytic fuel cell using visible light Ag_3PO_4/Fe/GTiP photoanode and $ZnIn_2S_4$ photocathode. J. Taiwan Inst. Chem. Eng. 96, 137–147.

Nahyoon, N.A., Liu, L., Rabe, K., Thebo, K.H., Yuan, L., Sun, J., Yang, F., 2018. Significant photocatalytic degradation and electricity generation in the photocatalytic fuel cell (PFC) using novel anodic nanocomposite of Fe, graphene oxide, and titanium phosphate. Electrochim. Acta 271, 41–48.

Nazir, A., Jariko, G.A., Junejo, M.A., 2013. Factors affecting sugarcane production in Pakistan.

Park, K.-H., Mondal, S., Ghosh, S., Das, S., Bhaumik, A., 2016. Enhanced efficiency in dye-sensitized solar cells based on mesoporous titanium phosphate photoanode. Microporous Mesoporous Mater. 225, 255–260.

Qureshi, A.L., Mahessar, A.A., Leghari, M.E.-U.-H., Lashari, B.K., Mari, F.M., 2015. Impact of releasing wastewater of sugar industries into drainage system of LBOD, Sindh, Pakistan. Int. J. Environ. Sci. Develop. 6 (5), 381.

Rabé, K., Liu, L., Nahyoon, N.A., Zhang, Y., Idris, A.M., 2019a. Enhanced Rhodamine B and coking wastewater degradation and simultaneous electricity generation via anodic g-C_3N_4/Fe^0 (1%)/TiO_2 and cathodic WO_3 in photocatalytic fuel cell system under visible light irradiation. Electrochim. Acta 298, 430–439.

Rabé, K., Liu, L., Nahyoon, N.A., Zhang, Y., Idris, A.M., 2019b. Visible-light photocatalytic fuel cell with Z-scheme g-C_3N_4/Fe^0/TiO_2 anode and WO_3 cathode efficiently degrades berberine chloride and stably generates electricity. Sep. Purif. Technol. 212, 774–782.

Rabé, K., Liu, L., Nahyoon, N.A., Zhang, Y., Idris, A.M., Sun, J., Yuan, L., 2019c. Fabrication of high efficiency visible light Z-scheme heterostructure photocatalyst g-C_3N_4/Fe^0 (1%)/TiO_2 and degradation of rhodamine B and antibiotics. J. Taiwan Inst. Chem. Eng. 96, 463–472.

Raizada, P., Kumari, J., Shandilya, P., Dhiman, R., Singh, V.P., Singh, P., 2017. Magnetically retrievable Bi_2WO_6/Fe_3O_4 immobilized on graphene sand composite for investigation of photocatalytic mineralization of oxytetracycline and ampicillin. Process Saf. Environ. Prot. 106, 104–116.

Raizada, P., Sudhaik, A., Singh, P., Hosseini-Bandegharaei, A., Thakur, P., 2019a. Converting type II AgBr/VO into ternary Z scheme photocatalyst via coupling with phosphorus doped g-C3N4 for enhanced photocatalytic activity. Sep. Purif. Technol., 115692

Raizada, P., Sudhaik, A., Singh, P., Shandilya, P., Gupta, V.K., Hosseini-Bandegharaei, A., Agrawal, S., 2019b. Ag_3PO_4 modified phosphorus and sulphur co-doped graphitic carbon nitride as a direct Z-scheme photocatalyst for 2, 4-dimethyl phenol degradation. J. Photochem. Photobiol., A 374, 22–35.

Raizada, P., Sudhaik, A., Singh, P., Shandilya, P., Saini, A.K., Gupta, V.K., Hosseini-Bandegharaei, A., 2019c. Fabrication of Ag_3VO_4 decorated phosphorus and sulphur co-doped graphitic carbon nitride as a high-dispersed photocatalyst for phenol mineralization and E. coli disinfection. Sep. Purif. Technol. 212, 887–900.

Raizada, P., Sudhaik, A., Singh, P., Shandilya, P., Thakur, P., Jung, H., 2020. Visible light assisted photodegradation of 2, 4-dinitrophenol using Ag_2CO_3 loaded phosphorus and sulphur co-doped graphitic carbon nitride nanosheets in simulated wastewater. Arabian J. Chem. 13, 3196–3209.

Reddy, S.S.G., Raju, A.S., Kumar, B.M., 2015. Phytoremediation of sugar industrial water effluent using various hydrophytes. Int. J. Environ. Sci. 5 (6), 1147.

Sahu, O., 2016. Treatment of industry wastewater using thermochemical combined processes with copper salt up to recyclable limit. Int. J. Sustain. Built Environ. 5 (2), 288–300.

Sahu, Omprakash, 2017. Treatment of sugar processing industry effluent up to remittance limits: Suitability of hybrid electrode for electrochemical reactor. MethodsX 4, 172–185.

Sahu, Omprakash et al, 2018. Treatment of sugar industry wastewater using a combination of thermal and electrocoagulation processes. International Journal of Sustainable Engineering 11 (1), 16–25.

Shandilya, P., Mittal, D., Soni, M., Raizada, P., Lim, J.-H., Jeong, D. Y., Singh, P., 2018. Islanding of EuVO4 on high-dispersed fluorine doped few layered graphene sheets for efficient photocatalytic mineralization of phenolic compounds and bacterial disinfection. J. Taiwan Inst. Chem. Eng. 93, 528–542.

Shivayogimath, C., Jahagirdar, R., 2013. Treatment of sugar industry wastewater using electrocoagulation technique. Int. J. Res. Eng. Technol. 1 (5), 262–265.

Singh, P., Priya, B., Shandilya, P., Raizada, P., Singh, N., Pare, B., Jonnalagadda, S., 2019. Photocatalytic mineralization of antibiotics using 60% WO_3/BiOCl stacked to graphene sand composite and chitosan. Arabian J. Chem. 12, 4627–4645.

Thebo, K.H., Qian, X., Zhang, Q., Chen, L., Cheng, H.-M., Ren, W., 2018. Highly stable graphene-oxide-based membranes with superior permeability. Nat. Commun. 9 (1), 1486.

Wang, W., Xiao, K., Zhu, L., Yin, Y., Wang, Z., 2017. Graphene oxide supported titanium dioxide & ferroferric oxide hybrid, a magnetically separable photocatalyst with enhanced photocatalytic activity for tetracycline hydrochloride degradation. RSC Adv. 7 (34), 21287–21297.

Wang, X., Yang, X., Cai, J., Miao, T., Li, L., Li, G., Wang, C., 2014. Novel flower-like titanium phosphate microstructures and their application in lead ion removal from drinking water. J. Mater. Chem. A 2 (19), 6718–6722.

Yang, J.-H., Zhang, K., Ma, D., 2013. Gourd-shaped silver nanoparticle–graphene composite for electrochemical oxidation of glucose. Mater. Lett. 97, 133–136.

Zhao, Y., Wei, Z., Pang, Q., Wei, Y., Cai, Y., Fu, Q., Liu, B., 2017. NASICON-Type $Mg_{0.5}Ti_2(PO_4)_3$ Negative electrode material exhibits different electrochemical energy storage mechanisms in Na-ion and Li-ion batteries. ACS Appl. Mater. Interfaces 9 (5), 4709–4718.